CHIN. PHYS. LETT. Vol. 36, No. 2 (2019) 020701

An Atomic Magnetometer with Spin-Projection Noise Proportional to $\sqrt{T_2}$ *

Hai-Feng Dong(董海峰)[1,2**], Xiao-Fei Wang(王笑菲)[1], Ji-Min Li(李继民)[1],
Jing-Ling Chen(陈静铃)[1], Yuan Ren(任元)[3]

[1]*School of Instrumentation and Optoelectronic Engineering, Beihang University, Beijing 100083*
[2]*Graduate School of China Academy of Engineering Physics, Beijing 100193*
[3]*Department of Aerospace Science and Technology, Space Engineering University, Beijing 101416*

(Received 12 September 2018)

There is a common sense view for atomic magnetometers that their spin-projection-noises (SPNs) are inversely proportional to $\sqrt{T_2}$, where T_2 is the transverse relaxation time. We analyze the current atomic magnetometer types and give a counter-example of this common sense, which is the all-optical spin precession modulated three-axis atomic magnetometer proposed by our group in 2015. Unlike the other atomic magnetometers, the SPN of this kind of atomic magnetometers is proportional to $\sqrt{T_2}$ due to the fact that the scale factor between P_x and B can be unrelated to the transverse relaxation time T_2. We demonstrate this irrelevance experimentally and analyze the SPN theoretically. Using short-pulse ultra-high power laser to fully polarize the atoms, the phenomenon that SPN decreases with T_2 may also be demonstrated experimentally and a new tool for researching SPN in atomic magnetometers may be realized.

PACS: 07.55.Ge, 32.30.Dx, 42.50.Lc DOI: 10.1088/0256-307X/36/2/020701

Spin projection noise is one of the fundamental noises of all the atomic magnetometers, which is usually inverse proportional to $\sqrt{T_2}$. Not that we said 'usually' here because we have recently found an exception. First, let us see how usual this inverse-proportion property really is.

In most cases, the dynamics of the spin polarization in atomic magnetometers can be well-described by the Bloch equations[1–3]

$$\frac{d\boldsymbol{P}}{dt} = \gamma \boldsymbol{P} \times \boldsymbol{B} + \frac{R_\mathrm{p}}{q}(\boldsymbol{s} - \boldsymbol{P}) - \frac{R_1, R_2}{q}\boldsymbol{P}, \quad (1)$$

where $\gamma = \gamma^\mathrm{e}/q$ is the atomic gyromagnetic ratio, γ^e is the gyromagnetic ratio of electron, $R_1 = R_\mathrm{sd} + qR_\mathrm{wall}$ is the longitudinal relaxation rate, $R_2 = R_1 + qR_\mathrm{se}/q_\mathrm{se} + qR_\mathrm{gr}$ is the transverse relaxation rate, R_p is the pumping rate, q is the slowing-down factor, and $\boldsymbol{B}$ is composed of B_x, B_y, B_z and $B_1 \sin(wt)$. These four components and the scalar B_0 can all be the measured magnetic fields.

Typically, two different atomic magnetometers can be used to measure B_1: the first is a radio-frequency atomic magnetometer (RF AM),[4–6] and the second is a spin-exchange relaxation free atomic magnetometer (SERF AM).[2,3,7–10] Thus, one may not be surprised to see that their optimized scale factor between magnetic field and spin polarization P_x at resonance is the same. The optimized scale factor of the former is close to $\frac{1}{2}\gamma T_2$ considering that $R_2 \gg R_1$ in the normal regime. That of the latter is also close to $\frac{1}{2}\gamma T_2$ when magnetic gradient is shielded and compensated, thus $R_1 \approx R_2$ in the SERF regime.[2] Although the scale factor of RF AM here has the same form with Eq. (1) in Ref. [4] we can obtain it by optimizing the pumping rate instead of supposing that the atoms are nearly completely polarized along z axis.

Considering the spin projection noise (SPN) of spin polarization P_x caused by Heisenberg uncertainty

$$\delta P_x = 2\sqrt{\frac{T_2}{qN}}, \quad (2)$$

where q is the slowing-down factor, $T_2 = q/(R_\mathrm{p} + R_2)$ is the transverse relaxation time, and N is the atom numbers. We can deduce both the equivalent magnetic field SPNs of the two atomic magnetometers are $\frac{4}{\gamma\sqrt{qNT_2}}$. It is clear that their SPNs are inversely proportional to $\sqrt{T_2}$.

Typically, three different magnetometers can be used to measure the scalar magnetic field B_0, which are M_x,[11] M_z,[12] and Bell–Bloom magnetometer.[13–15] For M_x AM, one needs to optimize the oscillation field amplitude B_1 and the pumping rate R_p at the same time. In the case when $R_2 \gg R_1$, the maximum scale factor for measuring B_0 using M_x AM is approximately $\frac{1}{2\sqrt{3}}\gamma T_2$. This result is different from Eq. (6) in Ref. [11] where only the field amplitude B_1 is optimized.

For M_z AM, the P_z signal has an absorption form, and the magnetic field modulation is needed for the synchronous detection. The maximum scale factor to measure B_0 using M_z AM is approximately $\frac{1}{4}\gamma T_2$. As far as we know, there are no other forms of optimization result for the scale factor of M_z AM.

*Supported by the National Natural Science Foundation of China under Grant Nos 51675034 and 61273067, and the Natural Science Foundation of Beijing Municipality under Grant No 7172123.
**Corresponding author. Email: hfdong@buaa.edu.cn
© 2019 Chinese Physical Society and IOP Publishing Ltd

Table 1. Scale factors between polarization and magnetic field, and SPNs of several typical atomic magnetometers ($\star$ means the same as the B_0-type scalar magnetometry).

AM types		Scale factor	SPN
B_1	RF	$\frac{1}{2}\gamma T_2$	$\frac{4}{\gamma\sqrt{qNT_2}}$
	SERF	$\frac{1}{2}\gamma T_2$	$\frac{4}{\gamma\sqrt{qNT_2}}$
	M_x	$\frac{1}{2\sqrt{3}}\gamma T_2$	$\frac{4\sqrt{3}}{\gamma\sqrt{qNT_2}}$
B_0	M_z	$\frac{1}{4}\gamma T_2$	$\frac{8}{\gamma\sqrt{qNT_2}}$
	Bell–Bloom	$\frac{1}{2}\gamma T_2$	$\frac{4}{\gamma\sqrt{qNT_2}}$
B_x, B_y, B_z	MScM	$\star$	$\star$
	MRoM	$\frac{1}{\sqrt{6}}\gamma T_2$, $\frac{1}{\sqrt{6}}\gamma T_2$, $\frac{1}{2\sqrt{3}}\gamma T_2$	$\frac{2\sqrt{6}}{\gamma\sqrt{qNT_2}}$, $\frac{2\sqrt{6}}{\gamma\sqrt{qNT_2}}$, $\frac{4\sqrt{3}}{\gamma\sqrt{qNT_2}}$
	MCoM	$\star$	$\star$
	MPrM	$\star$	$\star$
	MCrM	$\frac{\sqrt{2}}{4}\gamma T_2$, $\frac{1}{2}\gamma T_2$, $\frac{\sqrt{2}}{4}\gamma T_2$	$\frac{4\sqrt{2}}{\gamma\sqrt{qNT_2}}$, $\frac{4}{\gamma\sqrt{qNT_2}}$, $\frac{4\sqrt{2}}{\gamma\sqrt{qNT_2}}$
	MSeM	$\frac{3\sqrt{3}}{8}\gamma T_2$, $\frac{3\sqrt{3}}{8}\gamma T_2$, $\frac{9}{64}\gamma T_2$	$\frac{16\sqrt{3}}{9\gamma\sqrt{qNT_2}}$, $\frac{16\sqrt{3}}{9\gamma\sqrt{qNT_2}}$, $\frac{128}{9\gamma\sqrt{qNT_2}}$
	SMoM	$\star$, $\frac{1}{B_0}$, $\frac{1}{B_0}$	$\star$, $2B_0\frac{\sqrt{T_2}}{qN}$, $2B_0\frac{\sqrt{T_2}}{qN}$

For Bell–Bloom AM, $B_1 = 0$ and the resonance is realized through pulsed pumping. Only the pumping rate needs to be optimized and the maximum scale factor is $\frac{1}{2}\gamma T_2$.

By using these scale factors for M_x, M_z and Bell–Bloom magnetometers and Eq. (2), the equivalent magnetic field SPNs of these three magnetometers are deduced to be $\frac{4\sqrt{3}}{\gamma\sqrt{qNT_2}}$, $\frac{8}{\gamma\sqrt{qNT_2}}$ and $\frac{4}{\gamma\sqrt{qNT_2}}$, respectively. It is obvious that all of them are inverse proportional to $\sqrt{T_2}$. Note that although P_z is measured in M_z AM, we still use Eq. (2) for the SPN calculation because of the symmetry of the spin projection noise.

Finally, let us consider the measurement of magnetic field components; i.e., B_x, B_y and B_z. There are typically seven methods to realize three-axis vector atomic magnetometry.

The first is called magnetic field scanning magnetometry (MScM), which was proposed by Alldredge in the 1960s,[16,17] in which the field along a certain direction is scanned while the scalar field is monitored. The scanning field corresponding to the minimum of the scalar field is opposite to the field in the scanning direction. Because the vector field is measured directly by the scalar magnetometer, the equivalent magnetic field SPN is the same as that of the scalar magnetometer.

The second is magnetic field rotation magnetometry (MRoM), which was proposed by Vershovskii *et al.* in 2004,[18] in which the total field is locked by measuring and compensating the transverse fields. As the measurement of the total field B_0 is discussed above, here we focus on the scale factor and SPN of the transverse fields measurement. The transverse fields are measured by adding a rotation magnetic field perpendicular to the total field B_0. In this way, the total field will oscillate in the same frequency when there is a transverse field. The amplitude and phase of this oscillation are decided by the transverse field. Thus, one can measure the transverse fields through the measurement of B_0's oscillation. In the real application, B_1 is usually much smaller than B_0. Here, we just optimize the scale factor theoretically. If the scalar magnetometer has fast response to the direction change, the optimized scale factor happens when the modulation field is equal to B_0. It is enhanced by a factor of $\sqrt{2}$ from the B_0 measurement. Here, M_x is used more frequently for MRoM than the other B_0 magnetometers due to frequency response consideration. Thus, the optimized scale factor of B_x, B_y for MRoM is $\frac{1}{\sqrt{6}}\gamma T_2$, and that of B_z is the same as the M_x magnetometer.

The third is magnetic field compensation magnetometry (MCoM), which was proposed by Vershovskii in 2006,[19] in which two orthogonal fields are compensated for so that the measured scalar field is equal to the field along direction perpendicular to the previous two fields' directions. By carrying out the compensation successively, one can obtain the three-axis magnetic fields. This is a method with high accuracy due to the orthogonal between the measured field and the compensation field. From the viewpoint of SPN, it is the same as the scalar magnetometer.

The fourth is magnetic field projection magnetometry (MPrM), which was proposed by Patton *et al.* in 2014,[20] which measures the field direction by the projections of three-axis orthogonal fields. As the scalar field is measured directly, the equivalent field SPN is also the same as the scalar magnetometer.

The fifth is magnetic field cross-modulation magnetometer (MCrM), which was proposed by Seltzer and Romalis,[21] in which B_y is measured in the same way with the SERF magnetometer mentioned above, B_x and B_z are measured by cross modulation. Here, we focus on the transverse magnetic field B_x and B_z. After cross-modulation and lock-in amplifier, the scale

factor between output spin polarization and transverse magnetic field is $\frac{R_p}{R_p+R_2}\frac{B_m}{(\frac{R_p+R_2}{\gamma})^2+\frac{B_m^2}{2}}$, which has a maximum value of $\frac{\sqrt{2}}{4}\gamma T_2$.

The sixth is magnetic field separate modulation magnetometry (MSeM), in which three different modulation fields are added to three axes separately.[22] We proposed and verified the usage of MSeM in zero field in 2012,[9] and solved the key problems in 2016.[23] In this case, we deduced that the optimized scale factor of three axes are $\frac{3\sqrt{3}}{8}\gamma T_2$, $\frac{3\sqrt{3}}{8}\gamma T_2$, and $\frac{9}{64}\gamma T_2$, respectively.

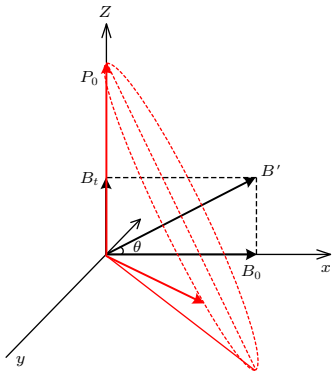

Fig. 1. Schematic diagram of the polarization measurement of spin precession modulated atomic magnetometer.

The seventh vector atomic magnetometer is spin modulation magnetometry (SMoM), which was pioneered by Fairweather and Usher in 1972.[24] In 2015, we proposed a kind of all-optical three-axis SMoM.[25] Furthermore, we recently find that this kind of atomic magnetometers has an abnormal property; i.e., their SPN is proportional to $\sqrt{T_2}$. The detailed sensing mechanism was described in Ref. [25]. Here we give a brief introduction for convenience of reading.

The principle of SMoM is shown in Fig. 1. Assuming that the initial magnetic field is parallel to the direction of the probe light (x axis), there is no projection of spin polarization along the probe beam. When a small transverse magnetic field (B_t) perpendicular to the direction of the probe beam appears, the direction of the total magnetic field is deviated from its initial position. As the deviation angle is small enough, the polarization oscillation amplitude in the direction of the probe beam can be approximately as $\frac{P_0}{B_0}$, which has a maximum value of $\frac{1}{B_0}$ for $P_0 = 1$.

Similar to the measurement of B_1 and B_0, we can also obtain the SPNs and B_x, B_y and B_z using Eq. (2) and the corresponding scale factors. In Table 1, we list all the magnetometers' optimized scale factors and SPNs. It is clearly shown that most of the atomic magnetometers are inverse-proportional to $\sqrt{T_2}$, which is the reason why it becomes a common sense. The only exception is SMoM. The basic reason for this phenomenon is that when all the other atomic magnetometers have optimized scale factors proportional to T_2, that of SMoM is unrelated to T_2 in the transverse direction. For the main field, it depends on the used scalar magnetometry, which may be Bell–Bloom[15] or M_x magnetometer.[24]

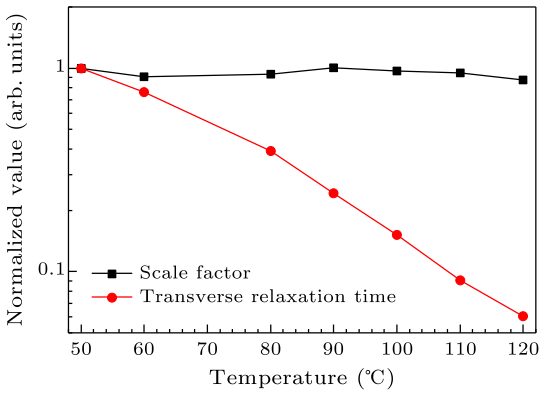

Fig. 2. Normalized relation between scale factor, T_2 and the cell temperatures. The black square points present the normalized scale factor between P_x and B. The red circular points present the normalized transverse relaxation time T_2. With the increase of temperature, T_2 decreases and the scale factor of SMoM is kept to be constant.

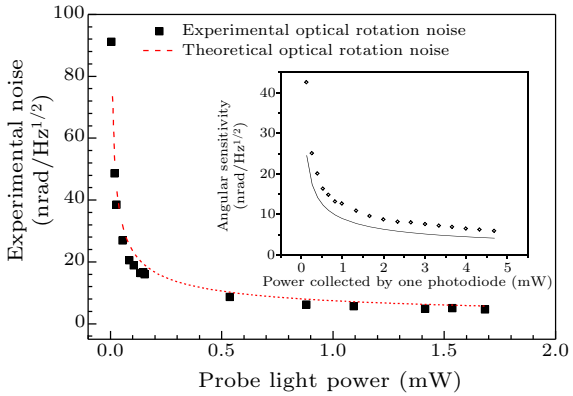

Fig. 3. The relationship between probe light power and optical rotation noise. The black square points present the optical rotation noise under variable probe light power. The red line is the fitting curve. Inset: the optical rotation characterization in Ref. [4].

We carry out an experiment to verify this irrelevance. The basic experimental setup is similar to our previous report,[25] and the only difference is that short pulse light is used for the synchronous pumping in this experiment instead of acoustic optical modulation. We change the cell temperature from 50℃ to 120℃. The transverse relaxation time T_2 is measured by the fitting of the free induced decay signal. Figure 2 shows the normalized transverse relaxation time and scale factor for different temperatures. From Fig. 2, we can see that when T_2 is shortened with the increase of the temperature, the scale factor is kept to be constant. As B_0 is the same for different temperatures, we know that the spin polarization is also kept constant.

We also calibrate the probe noise by blocking the

pumping beam, which is shown in Fig. 3. The black square is the optical rotation noise while the red line is photon shot noise calculated by $\delta\phi = \frac{1}{\sqrt{2\Phi\eta}}$, where Φ is the probe beam photons flux, and $\eta = 0.9$ is the photodiode quantum efficiency. The inset in Fig. 3 is the same measurement from Ref. [4] which is given for comparison. From Fig. 3, we can see that the probe noise is limited by photon shot noise, which is also the main noise source of the magnetometer. Thus, we have not observed the SPN and its variation with T_2 directly at the current stage.

In summary, we have classified atomic magnetometers into three types according to the measured field in the Bloch equation. Their optimized scale factors are analyzed one by one. Together with the variation of spin polarization, we deduce their equivalent magnetic field SPNs, respectively. Our analysis illustrates a general rule for atomic magnetometer's SPN; i.e., the SPN is inversely proportional to $\sqrt{T_2}$ and shows one counter-example at the same time. We analyze the reason for this unusual example and carry out experiments to verify the reason. As the noise is overwhelmed by the photon shot noise, the expected SPN's decrease with the shortening of T_2 is not observed directly. Using the high power short pulse pumping source, it is possible to fully polarize the atoms and achieve an atomic magnetometer limited by SPN. This may provide an experimental method for the research of SPNs in the atomic magnetometers. Meanwhile, once the sensitivity is dominated by SPN, this kind of special atomic magnetometers can improve the magnetic field sensitivity by decreasing instead of increasing T_2, which is much easier to be realized practically.

References

[1] Kornack T W and Romalis M V 2002 *Phys. Rev. Lett.* **89** 253002
[2] Allred J C, Lyman R N, Kornack T W and Romalis M V 2002 *Phys. Rev. Lett.* **89** 130801
[3] Ledbetter M P et al 2008 *Phys. Rev. A* **77** 033408
[4] Savukov I M, Seltzer S J, Romalis M V and Sauer K L 2005 *Phys. Rev. Lett.* **95** 063004
[5] Deans C, Marmugi L and Renzoni F 2017 *Opt. Express* **25** 17911
[6] Lee S K et al 2006 *Appl. Phys. Lett.* **89** 214106
[7] Shah V, Knappe S, Schwindt P D D and Kitching J 2007 *Nat. Photon.* **1** 649
[8] Johnson C, Schwindt P D D and Weisend M 2010 *Appl. Phys. Lett.* **97** 243703
[9] Dong H F et al 2012 *Eur. Phys. J. Appl. Phys.* **57** 21004
[10] Li R J et al 2017 *Chin. Phys. B* **26** 120702
[11] Smullin S J et al 2009 *Phys. Rev. A* **80** 033420
[12] Schultze V et al 2017 *Sensors* **17** 561
[13] Bell W E and Bloom A L 1957 *Phys. Rev.* **107** 1559
[14] Wang M B, Zhao D F, Zhang G Y and Zhao K F 2017 *Chin. Phys. B* **26** 100701
[15] Huang H C, Dong H F, Hao H J and Hu X Y 2015 *Chin. Phys. Lett.* **32** 098503
[16] Alldredge L R 1960 *J. Geophys. Res.* **65** 3777
[17] Alldredge L R and Ignas S 1964 *J. Geophys. Res.* **69** 1963
[18] Alexandrov E B et al 2004 *Meas. Sci. Technol.* **15** 918
[19] Vershovskii A K 2006 *Opt. Spectrosc.* **101** 309
[20] Patton B, Zhivun E, Hovde D C and Budker D 2014 *Phys. Rev. Lett.* **113** 013001
[21] Seltzer S J and Romalis M V 2004 *Appl. Phys. Lett.* **85** 4804
[22] Gravrand O, Khokhlov A, Mouel J L L and Leger J M 2001 *Earth Planets Space* **53** 949
[23] Huang H C, Dong H F, Chen L and Gao Y 2016 *Appl. Phys. Lett.* **109** 062404
[24] Fairweather A J and Usher M J 1972 *J. Phys. E* **5** 986
[25] Huang H C et al 2015 *Appl. Phys. Lett.* **107** 182403